Transp Porous Med (2012) 94:399–416
DOI 10.1007/s11242-012-0011-3

Thermal Stratification Effects on Hiemenz Flow of Nanofluid Over a Porous Wedge Sheet in the Presence of Suction/Injection Due to Solar Energy: Lie Group Transformation

R. Kandasamy · I. Muhaimin · N. Siva Ram · K. K. Sivagnana Prabhu

Received: 26 December 2011 / Accepted: 12 April 2012 / Published online: 26 April 2012

Abstract The objective of the present work is to investigate theoretically the Hiemenz flow and heat transfer of an incompressible viscous nanofluid past a porous wedge sheet in the presence of thermal stratification due to solar energy (incident radiation). The wall of the wedge is embedded in a uniform Darcian porous medium to allow for possible fluid wall suction or injection and has a power–law variation of the wall temperature. The partial differential equations governing the problem under consideration are transformed by a special form of Lie symmetry group transformations viz., one-parameter group of transformation into a system of ordinary differential equations which are solved numerically by Runge–Kutta–Gill-based shooting method. The conclusion is drawn that the flow field and temperature are significantly influenced by convective radiation, thermal stratification, buoyancy force, and porosity of the sheet.

Keywords Nanofluids · Porous wedge · Hiemenz flow · Thermal stratification and solar energy

1 Introduction

Sustainable energy generation is one of the most important challenges facing society today. Solar energy offers a solution with the hourly solar flux incident on the Earth's surface being greater than all the human consumption of energy in a year. Solar energy is one of the best sources of renewable energy with minimal environmental impact (Sharma et al. 2009). Power tower solar collectors could benefit from the potential efficiency improvements that arise from using a nanofluid as a working fluid. Although considerable attention has been placed on the

R. Kandasamy (✉) · I. Muhaimin
Research Centre for Computational Mathematics, FSTPI, Universiti Tun Hussein Onn Malaysia, Johor, Malaysia
e-mail: future990@gmail.com

N. S. Ram · K. K. S. Prabhu
RMK Engineering College, Anna University, Chennai, India

heat transfer enhancement capabilities of nanofluids, surprisingly, few authors seem to have an interest in quantifying potentially limiting factors (such as considerable increases in viscosity) that can decrease the overall benefits of the use of nanofluids in practical applications. The basic concept of using particles to collect solar energy was studied in the 1970s by Hunt (1978). Nanoparticles in the base fluid (nanofluid) provide the following possible advantages with respect to heat transfer in the solar energy absorb system: (1) nanofluids can absorb energy directly—skipping intermediate heat transfer steps, (2) the nanofluids can be optically selective (i.e., high absorption in the solar range and low emittance in the infrared), (3) a more uniform receiver temperature can be achieved inside the collector (reducing material constraints), (4) enhanced heat transfer via greater convection and thermal conductivity may improve receiver performance, and (5) absorption efficiency may be enhanced by tuning the nanoparticle size and shape to the Biomedicine application.

The study of heat transfer in the presence of nanofluids is of great practical importance to engineers and scientists because of its almost universal occurrence in many branches of science and engineering. A non-exhaustive list comprises the studies of Choi (1995), Buongiorno and Hu (2005), Buongiorno (2006), Kuznetsov and Nield (2010), Nield and Kuznetsov (2009) and Cheng and Minkowycz (1977). Numerous models and group theory methods have been proposed by different authors to study convective flows of nanofluids, e.g., Birkoff (1948, 1960), Yurusoy and Pakdemirli (1997, 1999b) and Yurusoy et al. (2001).

Convective flow in porous media has been widely studied in the recent years due to its wide applications in engineering as post-accidental heat removal in nuclear reactors, solar collectors, drying processes, heat exchangers, geothermal and oil recovery, building construction, etc. Chamkha and Khaled (2000) reported the effect of coupled heat and mass transfer by mixed convection in a linearly stratified stagnation flow (Hiemenz flow) in the presence of an externally applied magnetic field and internal heat generation or absorption. Seddeek et al. (2007) investigated the effects of chemical reaction and variable viscosity on hydrodynamic mixed convection heat and mass transfer for Hiemenz flow through porous media in the presence of an incident external magnetic field. Tsai and Huang (2009) investigated heat and mass transfer for Soret and Dufour's effects on Hiemenz flow through a porous medium onto a stretching surface. In their work, Abdel-Rahman (2010) numerically studied the effects of thermal diffusion and of an external applied magnetic field on a stagnation point flowing over a flat stretching surface taking into account variations of the viscosity under the Soret and Dufour's conditions.

The study of the stagnation flow problem was initiated by Hiemenz (1911) who developed an exact solution for the Navier-Stokes equations under a forced convective regime. Yih (1998) reported on the effects of uniform suction or blowing and magnetic field on the heat transfer characteristics of the Hiemenz problem in porous media. The effects of heat and mass transfer laminar boundary layer flow over a wedge have been studied by many authors Kafoussias and Nanousis (1997a,b), Anjali Devi and Kandasamy (2001), Yih (1998), Watanabe (1990), Chamkha and Khaled (2001), Hossian (1992), Hakiem et al. (1999), Kuo (2005) and Cheng and Lin (2002) in different situations.

In mixed nanoparticle flows of practical importance in science as well as in many engineering devices, the environment of the nanofluid is thermally stratified. The discharge of hot fluid into cold regions often results in a thermal stratification with lighter fluid overlying denser fluid. In particular, the study of heat transfer in the presence of thermal stratification is of considerable importance in chemical and hydrometallurgical industries. Nanofluids are suspensions of nanoparticles in fluids that show significant enhancement of their properties at modest nanoparticle concentrations. Many of the publications on nanofluids are about understanding their behavior so that they can be utilized where straight heat transfer enhancement

is paramount as in many industrial applications, nuclear reactors, transportation, electronics as well as biomedicine and food. In this new age of energy awareness, our lack of abundant sources of clean energy and the widespread dissemination of battery operated devices, such as cell-phones and laptops, have accented the necessity for a smart technological handling of energetic resources. Nanofluids have been demonstrated to be able to handle this role in some instances as a smart fluid.

Recently, the effect of chemical reaction and heat radiation in the presence of a nanofluid flowing past a porous vertical stretching surface was investigated by Rosmila et al. (2011). Kandasamy et al. (2011) analyzed the impact of thermophoresis particle deposition and Brownian diffusion motion on nanofluid in the presence of a magnetic field. They predicted that the magnitude of the magnetic field plays an important role on the nanoparticles in the presence of base fluids. Vajravelu et al. (2011) and Rana and Bhargava (2011) investigated the effects of heat transfer enhancement in mixed convection flow of a nanofluid along a vertical plate with heat source/sink. The two studies investigated the problem of mixed convection flow over a vertical plate, taking in to consideration the effects of the dependency of nanoparticle volume fraction depends on the shape of the same nanoparticles in the base fluid. The interest on Hiemenz flow in porous media has grown considerably in the last decades, since this geometry [geometry sounds weird] arises in many different systems, from natural to man-manufactured technological ones. The development of transport models in porous media had a bearing in the progress of several applications such as geology, chemical reactors, drying and liquid composite molding, combustion, and biological applications. In this review, the impact of the theory of transport in porous media on medical and biological sciences is discussed for different applications. Therefore, the fluid flow and heat transfer study in those systems is a subject of great interest in many branches of engineering and science. The governing equations of a fluid flow in a porous medium are non-linear and difficult to handle analytically. Consequently, problems concerning flows in porous medium are usually solved by numerical methods (Seddeek et al. 2007; Tsai and Huang 2009; Rosmila et al. 2011).

In this paper, we apply the so-called symmetry methods for a particular problem of fluid mechanics. The main advantage of such methods is that they can successfully be applied to non-linear differential equations. The symmetries of a differential equation are those continuous groups of transformations under which the differential equation remains invariant, that is, a symmetry group maps any solution to another solution. The interesting point is that, having obtained the symmetries of a specific problem, one can proceed further to find out the group-invariant solutions, which, in the case of the scaling group of transformations, are nothing but the well-known similarity solutions. The similarity solutions are quite popular because they result in the reduction of the independent variables of the problem. The method of Lie group transformations is used to derive all group-invariant similarity solutions of the unsteady two-dimensional laminar boundary-layer equations. On the other hand, it is now well known that the classical Lie symmetry method can be used to find similarity solutions, invariants, integrals motion, etc., systematically, see, for example, (Bluman and Kumei 1989; Ovsiannikov 1982; Ibragimov 1999 and the usefulness of this approach has been widely illustrated by several authors in different contexts such as; Yurusoy and Pakdemirli (1997, 1999b), Soh (2005), Hayat et al. (2005), Mohyuddin et al. (2004) and EL-Kabeir et al. (2008), and Avramenko et al. (2001) analyzed the application of Lie group theory to the boundary layers.

The goal of the present study is to analyze the development of the steady boundary layer flow and heat transfer over a porous wedge sheet in a nanofluid due to solar radiation. Lie symmetry group transformation is utilized to convert the governing partial differential equations into ordinary differential equations and then the numerical solution of the problem is

accomplished by Runge–Kutta–Gill method (1951) with shooting technique. This method has the following advantages over other available methods: (i) it utilizes less storage register, (ii) it controls the growth of rounding errors and is usually stable, and (iii) it is computationally economical. Numerical calculations were carried out for different values of dimensionless parameters of the problem under consideration for the purpose of illustrating the results graphically. The nanofluid is a colloidal suspension with nanoparticles dispersed uniformly in a base fluid and has many unique characteristics in thermal engineering fields. Solar energy is currently one kind of important resource for clean and renewable energy, and is widely investigated in many fields. In order to increase the operating temperature and thermodynamic efficiency, concentrated solar radiation is normally used to heat the working fluid in solar thermal power system. The study of heat transfer in the presence nanofluid past a porous plate due to solar energy is of great practical importance to engineers and scientists because of its almost universal occurrence in many branches of science and engineering. Possible applications of this type of flow can be found in many industries. Examination of such flow models reveals the influence of thermophoresis particle deposition and convective radiation on velocity and temperature profiles. For this reason, it is of special interest in this work to consider natural convection due to solar radiation flow from a wedge embedded in a porous medium with variable porosity distribution. The analysis of the results obtained shows that the flow field is influenced appreciably by the presence of convective radiation and thermophoresis particle deposition of the nanoparticles in the presence of nanofluid past a porous wedge sheet.

2 Mathematical Analysis

Consider the steady laminar two-dimensional flow of an incompressible viscous nanofluid past a porous wedge sheet in the presence of solar energy radiation (see, Fig. 1). The temperature at the wedge surface takes the constant value T_w, while the ambient value, attained as y tends to infinity, takes the constant value T_∞. Far away from the wedge plate, both the surroundings and the Newtonian absorbing fluid are maintained at a constant temperature T_∞.

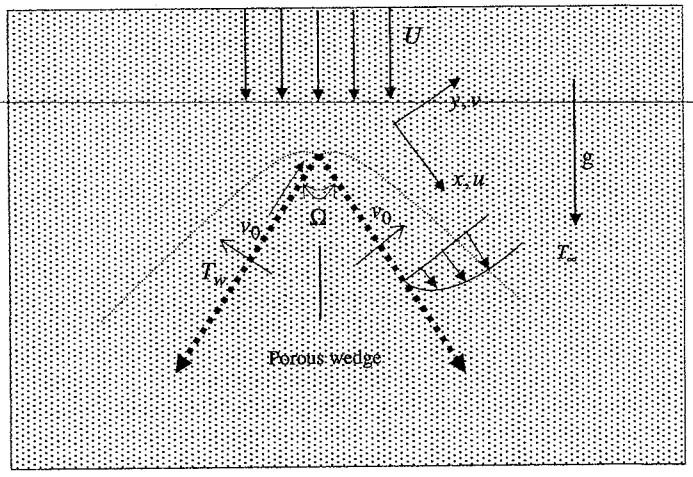

Fig. 1 Physical flow model over a porous wedge sheet

Table 1 Thermophysical properties of fluid and nanoparticles

	ρ(kg/m^3)	c_p(J/kg K)	k(W/mK)	$\beta \times 10^{-5}$(K^{-1})
Purewater ($\zeta = 0.0$)	997.1	4179	0.613	21
Copper (Cu) ($\zeta = 0.05$)	8933	385	401	1.67
Silver (Ag) ($\zeta = 0.01$)	10500	235	429	1.89
Alumina (Al_2O_3)($\zeta = 0.15$)	3970	765	40	0.85
Titanium (TiO_2)($\zeta = 0.2$)	4250	6862	8.9538	0.9

The porous medium is assumed to be transparent and in thermal equilibrium with the fluid. The thermal dispersion effect is minimal when the thermal diffusivity of the porous matrix is of the same order of magnitude as that of the working fluid. This viewpoint of assuming that the effective thermal diffusivity remains constant when the porosity of the porous medium varies with the normal distance is shared by many other investigators such as Vafai et al. (1985) and Tien and Hong (1985). The non reflecting absorbing in ideally transparent wedge plate receives an incident radiation flux of intensity q''_{rad}. This radiation flux penetrates the plate and is absorbed in an adjacent fluid of absorption coefficient (Fathalah and Elsayed 1980). Owing to heating of the absorbing nanofluid and the wedge plate by solar radiation, heat is transferred from the plate the surroundings. Also, the solar radiation is a collimated beam that is normal to the plate. The fluid is a water-based nanofluid containing Cu nanoparticles. As mentioned before, the working fluid is assumed to have heat absorption properties. For the present application, the porous medium absorbs the incident solar radiation and transits it to the working fluid by convection. The thermophysical properties of the nanofluid are given in Table 1 (see Oztop and Abu-Nada 2008). Under the above assumptions, the boundary layer equations governing the flow and thermal field can be written in dimensional form as

$$\frac{\partial \bar{u}}{\partial \bar{x}} + \frac{\partial \bar{v}}{\partial \bar{y}} = 0 \tag{1}$$

$$\bar{u}\frac{\partial \bar{u}}{\partial \bar{x}} + \bar{v}\frac{\partial \bar{u}}{\partial \bar{y}} = \frac{1}{\rho_{f_n}}\left[U\frac{dU}{dx}\rho_{f_n} + \mu_{f_n}\frac{\partial^2 \bar{u}}{\partial \bar{y}^2} + (\rho\beta)_{f_n}\bar{g}(T - T_\infty)\cos\frac{\Omega}{2} - \left(\frac{\nu_{f_n}}{K}\rho_{f_n}\right)(\bar{u} - U)\right] \tag{2}$$

$$\bar{u}\frac{\partial T}{\partial \bar{x}} + \bar{v}\frac{\partial T}{\partial \bar{y}} = \alpha_{f_n}\frac{\partial^2 T}{\partial \bar{y}^2} - \frac{1}{(\rho C_p)_{f_n}}\frac{\partial q''_{\text{rad}}}{\partial y} \tag{3}$$

Using Rosseland approximation for radiation (Sparrow and Cess (1978); Raptis (1998) and Brewster (1972)), we can write $q''_{\text{rad}} = -\frac{4\sigma_1}{3k^*}\frac{\partial T^4}{\partial y}$ where σ_1 is the Stefan–Boltzman constant, k^* is the mean absorption coefficient. The Rosseland approximation is used to describe the radiative heat transfer in the limit of the optically thick fluid (nanofluid).

The boundary conditions of these equations are

$$\bar{u} = 0, \bar{v} = -v_0, T = T_w + c_1 x^{n_1} \text{ at } \bar{y} = 0; \bar{u} \to U = cx^m, T \to T_\infty = (1-n)T_0 + nT_w \text{ as } \bar{y} \to \infty \tag{4}$$

where c, c_1 and n_1 (power index) are constants and V_0 and T_w are the suction (> 0) or injection (< 0) velocity and the fluid temperature at the plate. $\beta_1 = \frac{2m}{1+m}$ where β_1 is the Hartree pressure gradient parameter that corresponds to $\beta_1 = \frac{\Omega}{\pi}$ for a total angle Ω of the wedge,

The temperature of the fluid is assumed to vary following a power–law function while the free stream temperature is linearly stratified. In Eq. (4) and n is a constant parameter referred as the thermal stratification parameter, such that $0 \leq n < 1$. T_0 is a constant reference temperature say ($T_0 = T_\infty(0)$). The suffixes w and ∞ denote surface and ambient conditions. Here, c is a constant, $\bar{u}$ and $\bar{v}$ are the velocity components in the $\bar{x}$ and $\bar{y}$ directions, T is the local temperature of the nanofluid, $\bar{g}$ is the acceleration due to gravity, V_0 is the velocity of suction/injection, K is the permeability of the porous medium, ρ_{f_n} is the effective density of the nanofluid, q''_{rad} is the applied absorption radiation heat transfer, μ_{f_n} is the effective dynamic viscosity of the nanofluid, α_{f_n} is the thermal diffusivity of the nanofluid which are defined as (see Aminossadati and Ghasemi 2009),

$$\rho_{f_n} = (1-\zeta)\rho_f + \zeta\rho_s,\ \mu_{f_n} = \frac{\mu_f}{(1-\zeta)^{2.5}}$$
$$(\rho\beta)_{f_n} = (1-\zeta)(\rho\beta)_f + \zeta(\rho\beta)_s,\ \alpha_{f_n} = \frac{k_{f_n}}{(\rho C_p)_{f_n}},$$
$$(\rho c_p)_{f_n} = (1-\zeta)(\rho C_p)_f + \zeta(\rho c_p)_s$$

Maxwell model (1891) was developed to determine the effective electrical or thermal conductivity of liquid-solid suspensions. This model is applicable to statistically homogeneous and low volume concentration liquid-solid suspensions, with randomly dispersed and uniformly sized non-contacting spherical particles. It is given as

$$\frac{k_{f_n}}{k_f} = \left\{\frac{(k_s + 2k_f) - 2\zeta(k_f - k_s)}{(k_s + 2k_f) + 2\zeta(k_f - k_s)}\right\} \tag{5}$$

Experiments report thermal conductivity enhancement of nanofluids be yond the Maxwell limit of 3ζ. In the limit of low particle volume concentration (ζ) and the particle conductivity (k_s), being much higher than the base liquid conductivity (k_f), Eq. (5) can be reduced to Maxwell 3ζ limit as

$$k_{low} = \frac{k_{f_n}}{k_f} = 1 + 3\zeta \tag{5a}$$

Equation (5) represents the lower limit for the thermal conductivity of nanofluids and it can seen that in the limit where $\zeta = 0$ (no particles), Eq. (5a) yields $k_{low} = 1$ as expected.

Where k_f and k_s are the thermal conductivity of the base fluid and nanoparticle, respectively, ζ is the nanoparticle volume fraction, μ_f is the dynamic viscosity of the base fluid, β_f and β_s are the thermal expansion coefficients of the base fluid and nanoparticle, respectively, ρ_f and ρ_s are the density of the base fluid and nanoparticle, respectively, k_{f_n} is the effective thermal conductivity of the nanofluid and $(\rho C_p)_{f_n}$ is the heat capacitance of the nanofluid, which are defined by introducing the following non-dimensional variables

$$x = \frac{\bar{x}}{\sqrt{\frac{\nu_f}{c}}},\ x = \frac{\bar{y}}{\sqrt{\frac{\nu_f}{c}}},\ u = \frac{\bar{u}}{\sqrt{c\nu_f}},\ v = \frac{\bar{v}}{\sqrt{c\nu_f}} \text{ and } \theta = \frac{T - T_\infty}{T_w - T_\infty} \tag{6}$$

Equations (1)–(4) take the non-dimensional form

$$\frac{\partial u}{\partial x} + \frac{\partial v}{\partial y} = 0 \tag{7}$$

$$u\frac{\partial u}{\partial x}+v\frac{\partial u}{\partial y}=\frac{1}{\left(1-\zeta+\zeta\frac{\rho_s}{\rho_f}\right)}\left[U\frac{dU}{dx}\frac{\rho_{f_n}}{\rho_f}+\frac{1}{(1-\zeta)^{2.5}}\frac{\partial^2 u}{\partial y^2}\right.$$
$$\left.+\left\{\left(1-\zeta+\zeta\frac{(\rho\beta)_s}{(\rho\beta)_f}\right)\gamma\cos\frac{\Omega}{2}\theta\right\}-\left(\frac{\lambda}{(1-\zeta)^{2.5}}\right)(u-U)\right] \tag{8}$$

$$u\frac{\partial\theta}{\partial\bar{x}}+v\frac{\partial\theta}{\partial\bar{y}}=\frac{1}{\Pr}\frac{1}{1-\zeta+\zeta\frac{(\rho c_p)_s}{(\rho C_p)_f}}\left[\frac{k_{f_n}}{k_f}\frac{\partial^2\theta}{\partial y^2}+\frac{4}{3}N\left\{(C_T+\theta)^3\theta'\right\}'\right] \tag{9}$$

with the boundary conditions

$$\bar{u}=0,\bar{v}=-V_0,T=T_w \text{ at } \bar{y}=0;\bar{u}\to U=cx^m,T\to T_\infty\to(1-n)T_o$$
$$+nT_w \text{ as } \bar{y}\to\infty \tag{10}$$

where $\Pr=\frac{\nu_f}{\alpha_f}$ is the Prandtl number, $\lambda=\frac{\nu_f}{cK}$ is the porous media parameter, $\gamma=\frac{gx(\rho\beta)_f\Delta T}{\rho_f U^2}$ is the buoyancy or natural convection parameter, $N=\frac{4\sigma_1\theta_w^3}{k_f k^*}$ is the conductive radiation parameter and $C_T=\frac{T_\infty}{T_w-T_\infty}$ is the temperature ratio where C_T assumes very small values by its definition as T_w-T_∞ is very large compared to T_∞. In the present study, it is assigned the value 0.1. It is worth mentioning that $\gamma>0$ aids the flow and $\gamma<0$ opposes the flow, while $\gamma=0$, i.e., (T_w-T_∞) represents the case of forced convection flow. On the other hand, if γ is of a significantly greater order of magnitude than one, then the buoyancy forces will be predominant. Hence, combined convective flow exists when $\gamma=O(1)$.

Following the lines of Kafoussias and Nanousis (1997a,b), the changes of variables are

$$\eta=\sqrt{\frac{(m+1)U}{2\nu x}}y,\psi=\sqrt{\frac{2\nu xU}{m+1}}f \text{ and } \theta=\frac{T-T_\infty}{T_w-T_\infty}$$

By introducing the stream function ψ, which defined as $u=\frac{\partial\psi}{\partial y}$ and $v=-\frac{\partial\psi}{\partial x}$, then the system of Eqs. (7)–(9) become

$$\frac{\partial\psi}{\partial y}\frac{\partial^2\psi}{\partial x\partial y}-\frac{\partial\psi}{\partial x}\frac{\partial^2\psi}{\partial y^2}=\frac{1}{\left(1-\zeta+\zeta\frac{\rho_s}{\rho_f}\right)}\left[U\frac{dU}{dx}\frac{\rho_{f_n}}{\rho_f}+\frac{1}{(1-\zeta)^{2.5}}\frac{\partial^3\psi}{\partial y^3}\right. \tag{11}$$
$$\left.+\left\{\left(1-\zeta+\zeta\frac{(\rho\beta)_s}{(\rho\beta)_f}\right)\gamma\cos\frac{\Omega}{2}\theta\right\}-\left(\frac{\lambda}{(1-\zeta)^{2.5}}\right)\left(\frac{\partial\psi}{\partial y}-U\right)\right]$$

$$\frac{\partial\psi}{\partial y}\frac{\partial\theta}{\partial x}-\frac{\partial\psi}{\partial x}\frac{\partial\theta}{\partial\bar{y}}=\frac{1}{\Pr}\frac{1}{1-\zeta+\zeta\frac{(\rho C_p)_s}{(\rho C_p)_f}}\left[\frac{k_{f_n}}{k_f}\frac{\partial^2\theta}{\partial y^2}+\frac{4}{3}N\left\{(C_T+\theta)^3\theta'\right\}'\right] \tag{12}$$

with the boundary conditions

$$\frac{\partial\psi}{\partial y}=0,\frac{\partial\psi}{\partial x}=-V_0,T=T_w \text{ at } y=0;\frac{\partial\psi}{\partial y}\to cx^m,T\to T_\infty\to(1-n)T_o$$
$$+nT_w \text{ as } \bar{y}\to\infty \tag{13}$$

The symmetry groups of Eqs. (11) and (12) are calculated by classical Lie group approach. The one-parameter infinitesimal Lie group of transformations leaving (11) and (12) invariant is defined as

$$x^*=x+\varepsilon\xi_1(x,y,\psi,\theta),y^*=y+\varepsilon\xi_2(x,y,\psi,\theta),$$
$$\psi^*=\psi+\varepsilon\mu_1(x,y,\psi,\theta),\theta^*=\theta+\varepsilon\mu_2(x,y,\psi,\theta) \tag{14}$$

From the algebraic technique, it is noticed that the form of infinitesimals as

$$\xi_1 = c_1 x + c_2, \xi_2 = g(x), \mu_1 = c_3\psi + c_4 \text{ and } \mu_2 = c_5\theta \tag{15}$$

where $g(x)$ is an arbitrary function.

Definitions of infinitesimal generators are

$$X_1 = x\frac{\partial}{\partial x} + g(x)\frac{\partial}{\partial y} + \psi\frac{\partial}{\partial \psi} + \theta\frac{\partial}{\partial \theta}, X_2 = \frac{\partial}{\partial x} + g(x)\frac{\partial}{\partial y}, X_3 = g(x)\frac{\partial}{\partial y} + \frac{\partial}{\partial \psi} \tag{16}$$

The partial differential equations governing the problem under consideration are transformed by a special form of Lie symmetry group transformations, viz., one-parameter infinitesimal Lie group of transformation into a system of ordinary differential equations. For the present case, the generator X_1 with $g(x) = 0$ is taken. The characteristic equations are

$$\frac{dx}{x} = \frac{dy}{0} = \frac{d\psi}{\psi} = \frac{d\theta}{\theta} \tag{17}$$

Solving the above equations, we get

$$\eta = y, \psi = xf(\eta) \text{ and } \theta = x\theta(\eta) \tag{18}$$

With the help of these relations, the (11) and (12) become

$$\begin{aligned} & f''' - \frac{2}{m+1}(1-\zeta)^{2.5}\xi^2 \\ & \times \left[\frac{\left(\frac{\lambda}{(1-\zeta)^{2.5}}\right)(f'-1) - m - \xi^2\left\{\left(1-\zeta+\zeta\frac{(\rho C_p)_s}{(\rho C_p)_f}\right)\right\}\gamma\cos\frac{\Omega}{2}\theta}{\left(1-\zeta+\zeta\frac{\rho_s}{\rho_f}\right)}\right] \\ & -\left(1-\zeta+\zeta\frac{\rho_s}{\rho_f}\right)(1-\zeta)^{2.5} \\ & \times\left[\frac{2m}{m+1}f'^2 - ff'' + \frac{1-m}{1=m}\xi\frac{\partial f}{\partial \xi}\left(\frac{\partial f}{\partial \eta} - \frac{\partial^2 f}{\partial \eta^2}\right)\right] = 0 \end{aligned} \tag{19}$$

$$\begin{aligned} & \theta'' + \frac{4}{3}\frac{k_f}{k_{f_n}}N\left\{(C_T+\theta)^3\theta'\right\} \\ & -\Pr\left\{1-\zeta+\zeta\frac{(\rho C_p)_s}{(\rho C_p)_f}\right\}\frac{k_f}{k_{f_n}} \\ & \times\left[\frac{2n_1}{m+1}\left[\theta+\frac{n}{1-n}\right]f' - f\theta' + \frac{1-m}{1+m}\left\{\xi\frac{\partial\theta}{\partial\xi}\frac{\partial f}{\partial\eta} - \xi\frac{\partial f}{\partial\xi}\frac{\partial\theta}{\partial\eta}\right\}\right] = 0 \end{aligned} \tag{20}$$

The boundary conditions take the following form

$$\frac{\partial f}{\partial \eta} = 0, \frac{m+1}{2}f + \frac{1-m}{2}\xi\frac{\partial f}{\partial \xi} = -S, \theta = 1 \text{ at } \eta = 0 \text{ and } \frac{\partial f}{\partial \eta} = 1, \theta \to 0 \text{ as } \eta \to \infty \tag{21}$$

where S is the suction parameter if $S > 0$ and injection if $S < 0$ and $\xi = kx^{\frac{1-m}{2}}$ Kafoussias and Nanousis (1997a,b), is the dimensionless distance along the wedge ($\xi > 0$). In this system of equations, it is obvious that the nonsimilarity aspects of the problem are embodied in the terms containing partial derivatives with respect to ξ. This problem does not admit similarity solutions. Thus, with ξ-derivative terms retained in the system of equations, it

is necessary to employ a numerical scheme suitable for partial differential equations for the solution. Formulation of the system of equations for the local nonsimilarity model with reference to the present problem will now be discussed.

At the first level of truncation, the terms accompanied by $\xi\frac{\partial}{\partial\xi}$ are small. This is particularly true when ($\xi \ll 1$). Thus, the terms with $\xi\frac{\partial}{\partial\xi}$ on the right-hand sides of Eqs. (19) and (20) are deleted to get the following system of equations:

$$f''' - \frac{2}{m+1}(1-\zeta)^{2.5}\xi^2 \times \left[\frac{\left(\frac{\lambda}{(1-\zeta)^{2.5}}\right)(f'-1) - m - \xi^2\left\{\left(1-\zeta+\zeta\frac{(\rho C_p)_s}{(\rho C_p)_f}\right)\right\}\gamma\cos\frac{\Omega}{2}\theta}{\left(1-\zeta+\zeta\frac{\rho_s}{\rho_f}\right)}\right] - \left(1-\zeta+\zeta\frac{\rho_s}{\rho_f}\right)(1-\zeta)^{2.5}\left[\frac{2m}{m+1}f'^2 - ff''\right] = 0 \tag{22}$$

$$\theta'' + \frac{4}{3}\frac{k_f}{k_{f_n}}N\left\{(C_T+\theta)^3\theta'\right\}' - \Pr\left\{1-\zeta+\zeta\frac{(\rho C_p)_s}{(\rho C_p)_f}\right\}\frac{k_f}{k_{f_n}}\left[\frac{2n_1}{m+1}\left[\theta+\frac{n}{1-n}\right]f' - f\theta'\right] = 0 \tag{23}$$

The boundary conditions take the following form

$$f' = 0, f = -\frac{2S}{m+1}, \theta = 1 \text{ at } \eta = 0 \text{ and } f' = 1, \theta \to 0 \text{ as } \eta \to \infty \tag{24}$$

For practical purposes, the functions $f(\eta)$ and $\theta(\eta)$ allow us to determine the skin friction coefficient

$$C_f = \frac{\mu_{f_n}}{\rho_f U^2}\left(\frac{\partial u}{\partial y}\right)_{aty=0} = -\frac{1}{(1-\zeta)^{2.5}}(\mathrm{Rex})^{-\frac{1}{2}}f''(0) \tag{25}$$

and the Nusselt number

$$Nu_x = \frac{xk_{f_n}}{k_f(T_w - T_\infty)}\left(\frac{\partial T}{\partial y}\right)_{aty=0} = -(\mathrm{Rex})^{\frac{1}{2}}\frac{k_{f_n}}{k_f}\theta'(0)\left[1+\frac{4}{3}N(C_T+\theta(0))^3\right] \tag{26}$$

respectively. Here, $\mathrm{Re}_x = \frac{Ux}{\nu_f}$ is the local Reynolds number.

3 Numerical Solution

The set of nonlinear ordinary differential Eqs. (22) and (23) with boundary conditions (24) have been solved by the Runge–Kutta–Gill method (1951) in conjunction with shooting technique with Pr, ζ, λ, n, n_1, S, Ω and N as prescribed parameters. The computations were done by a computer program which uses a symbolic and computational computer language MATLAB. A step size of $\Delta\eta = 0.001$ was selected to be satisfactory for a convergence criterion of 10^{-6} in nearly all cases. The value of η_∞ was found to each iteration loop by assignment statement $\eta_\infty = \eta_\infty + \Delta\eta$. The maximum value of η_∞ to each group of parameters Pr, ζ, λ, n, n_1, S, Ω and N determined when the values of unknown boundary conditions at $\eta = 0$ not change to successful loop with error less than 10^{-6}. Effects of heat transfer and

nanoparticle volume fraction on nanofluid over a porous wedge sheet in the presence of thermal stratification due to solar energy are studied for different values of thermal stratification and convective radiation. In the following section, the results are discussed in detail.

4 Results and Discussion

Equations (22) and (23) subjected to the boundary conditions (24) have been solved numerically for some values of the governing parameters Pr, $\zeta, m, \lambda, \gamma, n, n_1$ and N by Runge–Kutta–Gill algorithm with shooting technique. The case $\gamma \gg 1.0$ corresponds to pure free convection, $\gamma = 1.0$ corresponds to mixed convection, and $\gamma \ll 1.0$ corresponds to pure forced convection. Throughout this calculation, we have considered $\gamma = 2.0$ unless otherwise specified. The results for $-\theta'(0)$ are compared with those obtained by Lai and Kulacki (1990) and Yih (1998) for different values of S in Table 2. It can be seen that reasonably good agreement has been achieved for each values of S.

In the absence of energy equation, to ascertain the accuracy of our numerical results, the present study is compared with the available exact solution in the literature. The velocity profiles for different values of m are compared with the available exact solution of Schlichting (1979), is shown in Fig. 2. It is observed that the agreement with the theoretical solution of velocity profile is excellent.

Figures 3 and 4 illustrate typical temperature profiles as obtained by varying the thermal stratification parameter for the case of pure water (Fig. 3) and Cu–water (Fig. 4), respectively. It is clearly shown that the temperature of the fluid gradually decreases from higher value to the lower value only when the strength of thermal stratification is higher than the nanoparticles' volume fraction parameter because the size of the nanoparticles plays an important role on the motion of the fluid. For heat transfer characteristics mechanism, interesting result is the large distortion of the temperature field caused for $0.9 \leq n < 1$ ($n = 0$ refers flow at the wall, bottom layer and $n = 1$ refers flow at ambient, upper layer). In the case of pure water, negative value of the temperature profile characterizes the outer boundary region for $n = 0.9$, whereas for Cu water, negative value of the temperature profile occurs in the outer boundary region for $0.5 \leq n \leq 0.9$. It is noticed from the Figs. 3 and 4 that the temperature of the nanofluid (Cu–water) decreases significantly as compared to the pure water because the kinematic viscosity of the nanofluid is higher than the pure water. It is revealed from Figs. 5 and 6 that the temperature is enhanced by increasing the angle of inclination. The reason of the modeled temperature increase is that as the angle of inclination increases the effect of the buoyancy force due to thermal diffusion decreases by a factor of $\cos \frac{\Omega}{2}$. Consequently, the driving force of the fluid decreases and as a result

Table 2 Comparison of results for $-\theta'(0)$ with previous published works

S	Lai and Kulacki (1990)	Yih (1998)	Presentwork Pr = 1.0, $n = N = \zeta = 0, \Omega = 0$
−1.0	0.7766	0.776625	0.776638
−0.5	0.9909	0.990908	0.990913
0.00	1.2533	1.253298	1.253305
0.50	1.5599	1.559856	1.559863
1.00	1.9043	1.904254	1.904267

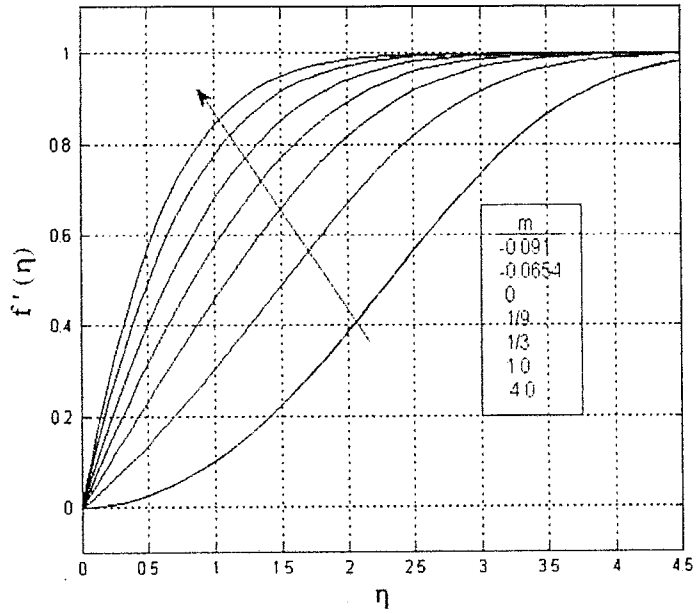

Fig. 2 Effects of m on the velocity distribution in the laminar flow past a wedge

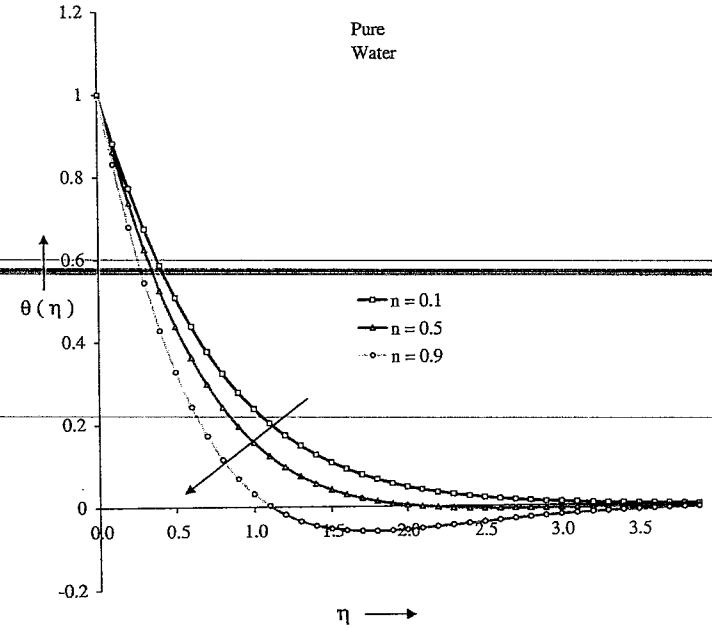

Fig. 3 Effect of thermal stratification over the temperature profiles. Pr $= 6.2, \zeta = 0.00, S = 1.0, \gamma = 2.0, N = 0.5, \lambda = 1.0, \xi = 0.01$ and $m = 0.0909(\Omega = 30°)$

the temperature increases. From Figs. 5 and 6, it is observed that the thermal boundary layer thickness of the nanofluid is stronger than the base fluid as the angle of inclination increases. Increasing the inclination angle makes it harder for the fluid to flow along the

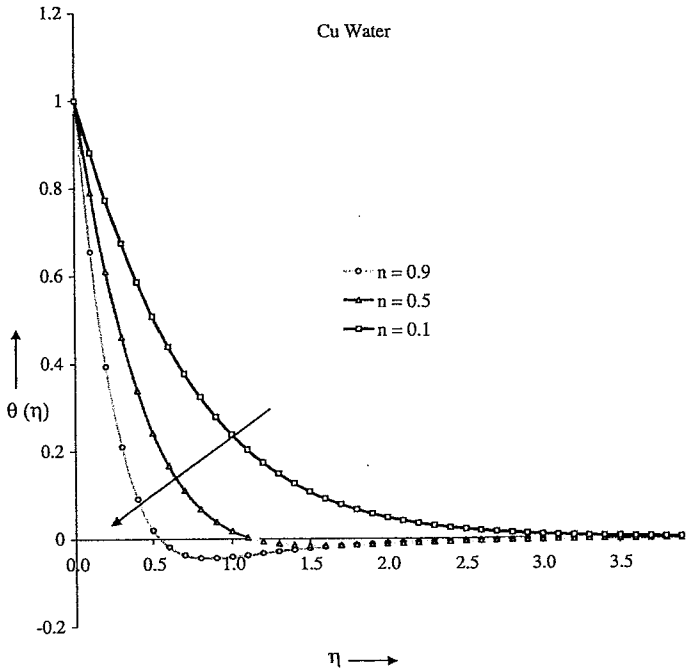

Fig. 4 Effect of thermal stratification over the temperature profiles. Pr $= 6.2, \zeta = 0.05, S = 1.0, \gamma = 2.0, N = 0.5, \lambda = 1.0, \xi = 0.01$ and $m = 0.0909(\Omega = 30°)$

plate and causes it to become warmer because the density of the nanofluid is higher than the pure water. This is due to the reduction in the thermal buoyancy effect caused by increase in θ. Further, it is observed from the Figs. 5 and 6 that the temperature of a nanofluid is remarkably lower as compared to that of the base fluid. Because the plate is inclined from vertical to horizontal, the buoyancy effect on the momentum and temperature profiles increases. This is because the incident solar radiation is initially absorbed by the absorbing fluid-matrix system which, in turn, heats up the ideally transparent plate. This operation of passing the absorbing fluid through an absorbing porous medium is believed to enhance solar collection by direct absorption in which heat losses are reduced as a result of plate temperatures.

Figures 7 and 8 display the effects of volume fraction of the nanoparticles on the velocity and temperature distribution, respectively. In the presence of uniform convective radiation, it is to note that the velocity of the fluid decreases, whereas the temperature of the fluid increases with increase of the nanoparticle volume fraction parameter, ζ. This agrees with the physical behavior that when the volume fraction of copper increases, the thermal conductivity and then the thermal boundary layer thickness increases. Changes in the size, shape, material, and volume fraction of the nanoparticles allow for tuning to maximize spectral absorption of solar energy throughout the fluid volume because the nanoparticle volume fraction parameter depends on the size of the particles. Enhancement in thermal conductivity can lead to efficiency improvements, although small, via more effective fluid heat transfer. Vast enhancements are found in surface area due to the extremely small particle size, which makes nanofluid-based solar systems attractive for thermochemical and photocatalytic processes. Figures 9 and 10 present the characteristic temperature

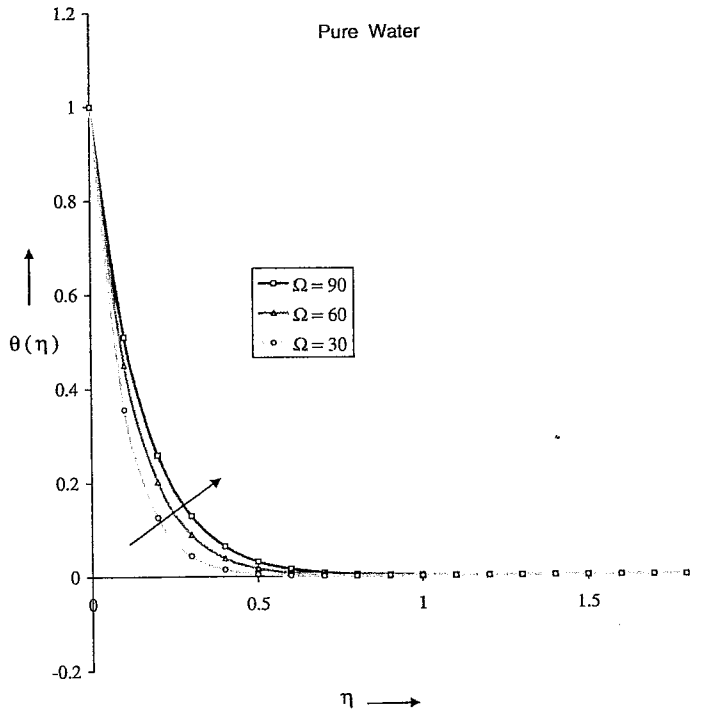

Fig. 5 Effect of thermal stratification over the temperature profiles. $\Omega\,\mathrm{Pr} = 6.2, \zeta = 0.00, S = 1.0, \gamma = 2.0, N = n = 0.5, \lambda = 1.0, \xi = 0.01, m = 0.20(\Omega = 60°), 0.333(\Omega = 90°)$ and $0.50(\Omega = 120°)$

profiles for different values of the convective radiation parameter N in the presence of base fluid (pure water) and nanofluid (Cu–water). According to Eqs. (2) and (3), the divergence of the radiative heat flux $\frac{\partial q''_{\mathrm{rad}}}{\partial y}$ increases as thermal conductivity of the fluid (k_f) decreases which in turn increases the rate of radiative heat transferred to the nanofluid and hence the fluid temperature decreases. In view of this explanation, the effect of convective radiation becomes more significant as $N \to 0 (N \neq 0)$ and can be neglected when $N \to \infty$. It is noticed that the temperature decreases with increase of the radiation parameter N. The effect of radiation parameter N is to reduce the temperature significantly in the flow region. Further, it is noticed that the temperature of a nanofluid is decelerated significantly as compared to the base fluid. All these physical behavior are due to the combined effect of porous strength of the wedge sheet and thermal conductivity of the nanofluid.

5 Conclusions

Influence of the different type of nanoparticles on Hiemenz boundary layer flow and heat transfer of incompressible Cu–water nanofluid along a porous wedge sheet in the presence of thermal stratification due to solar energy have been analyzed. Thermal boundary layer thickness of nanofluid is stronger than the base fluid as the angle of inclination increases because the driving force to the fluid decreases, and as a result temperature profiles increase. It is also

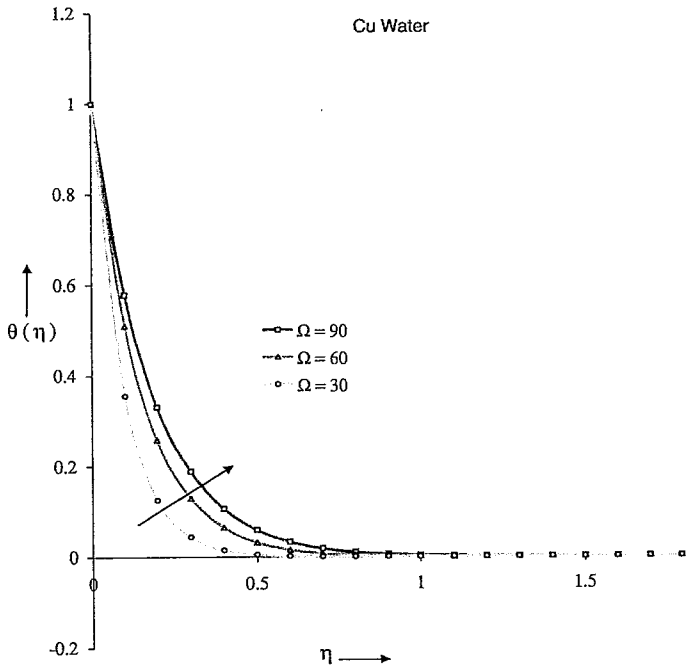

Fig. 6 Temperature profiles for various values of Ω. Pr $= 6.2, \zeta = 0.05, S = 1.0, \gamma = 2.0, N = n = 0.5, \lambda = 1.0, \xi = 0.01, m = 0.20(\Omega = 60°), 0.333(\Omega = 90°)$ and $0.50(\Omega = 120°)$

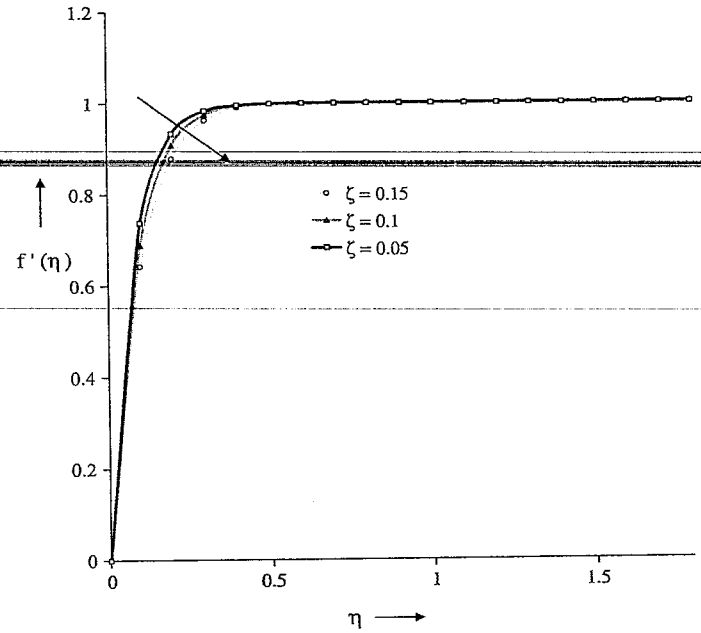

Fig. 7 Velocity profiles for various values of ζ. Pr $= 6.2, S = 1.0, \gamma = 2.0, N = n = 0.5, \lambda = 1.0, \xi = 0.01$ and $m = 0.0909(\Omega = 30°)$

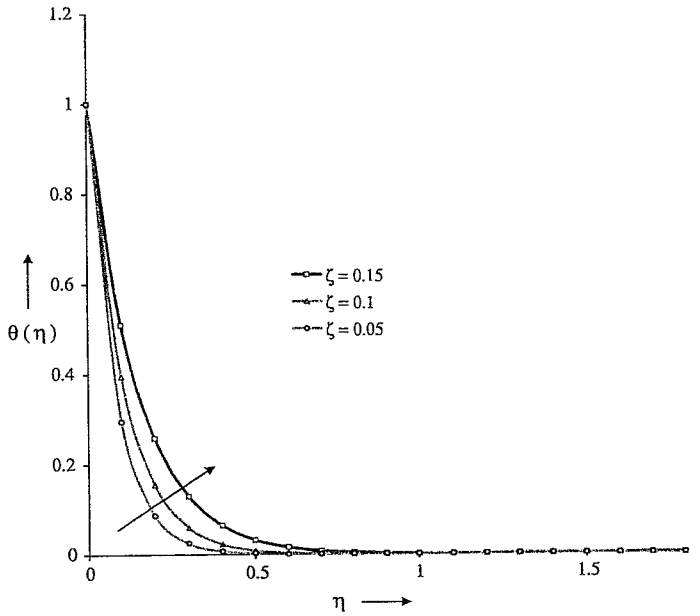

Fig. 8 Temperature profiles for various values of ζ. Pr $= 6.2, S = 1.0, \gamma = 2.0, N = n = 0.5, \lambda = 1.0, \xi = 0.01$ and $m = 0.0909(\Omega = 30°)$

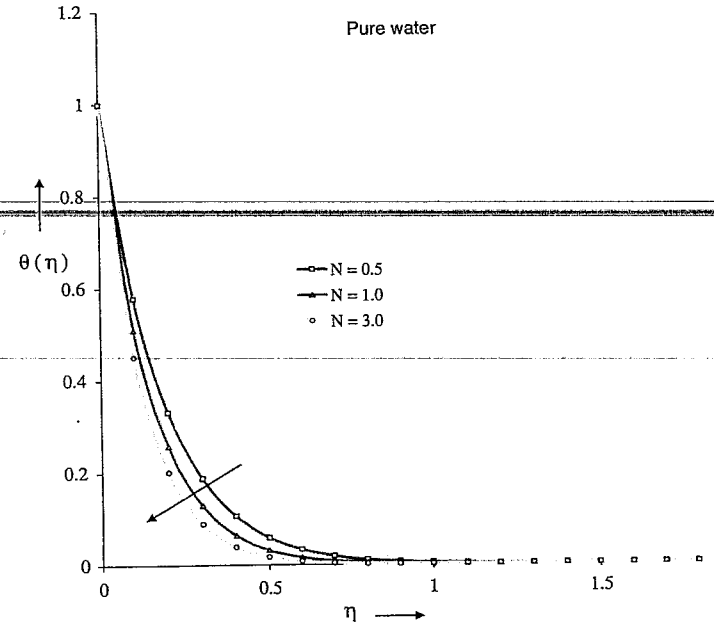

Fig. 9 Effect of Convective radiation over the temperature profiles. Pr $= 6.2, \zeta = 0.05, S = 1.0, \gamma = 2.0, n = 1.0, \lambda = 1.0, \xi = 0.01$ and $m = 0.0909(\Omega = 30°)$

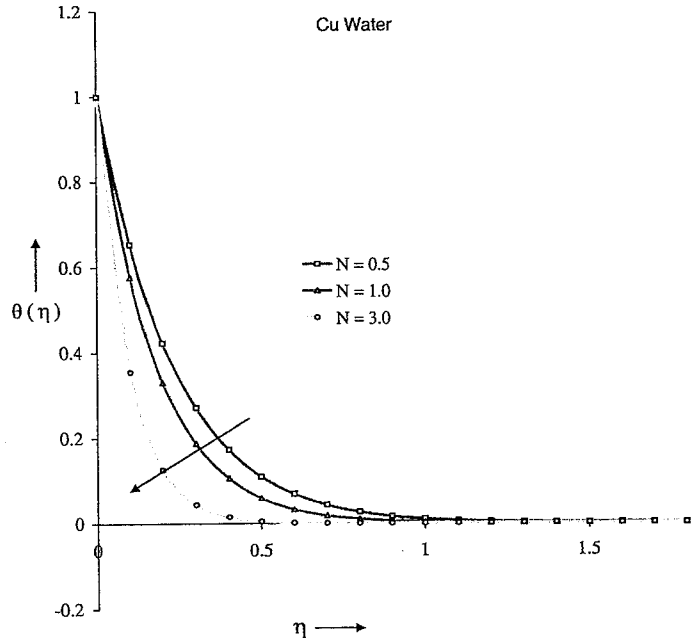

Fig. 10 Effect of convective radiation over the temperature profiles. Pr $= 6.2, \zeta = 0.05, S = 1.0, \gamma = 2.0, n = 0.5, \lambda = 1.0, \xi = 0.01$ and $m = 0.0909(\Omega = 30°)$

noticed that the temperature of a nanofluid is decelerated significantly as compared to the base fluid with increase of convective radiation. It is interesting to note that the thermal conductivity of the nanofluid also offers the potential of improving the radiative properties of the liquids, leading to an increase in the efficiency of direct absorption solar collectors. Decrease of momentum and increase of thermal boundary layer field due to increase in nanoparticle volume fraction parameter shows that the velocity increases and the temperature decreases gradually as we replace copper, $\zeta = 0.05$ by silver, $\zeta = 0.1$ and alumina, $\zeta = 0.15$ in the said sequence. In the presence of uniform nanoparticle volume fraction parameter, it is observed that the temperature of the Cu–water nanofluid is decreased significantly as compared to that of the base fluid with increase of thermal stratification and convective radiation parameter, respectively.

It is interesting to predict that the temperature of the nanofluid (Cu–water) decreases significantly as compared to the base fluid (pure water) with increase of thermal stratification effects. It has been shown that mixing nanoparticles in a liquid has a dramatic effect on the liquid thermophysical properties such as thermal conductivity of the nanofluid. Hiemenz flow over a porous wedge plate plays a very significant role on absorbs the incident solar radiation and transits it to the working fluid by convection. Nanofluids due to solar energy are important because they can be used in numerous applications involving heat transfer and other applications such as in detergency, solar collectors, drying processes, heat exchangers, geothermal and oil recovery, building construction, etc. The interdisciplinary nature of nanofluid research presents a great opportunity for exploration and discovery at the frontiers of nanotechnology. It is hoped that the present work will serve as a stimulus for needed experimental work on this problem.

References

Abdel-Rahman, G.M.: Thermal-diffusion and MHD for Soret and Dufour's effects on Hiemenz flow and mass transfer of fluid flow through porous medium onto a stretching surface. Phys. B **405**, 2560–2569 (2010)

Aminossadati, S.M., Ghasemi, B.: Natural convection cooling of a localized heat source at the bottom of a nanofluid-filled enclosure. Eur. J. Mech. B. Fluids **28**, 630–640 (2009)

Anjali Devi, S.P., Kandasamy, R.: Effects of heat and mass transfer on MHD laminar boundary layer flow over a wedge with suction or injection. J. Energy Heat Mass Transf. **23**, 167–178 (2001)

Avramenko, A.A., Kobzar, S.G., Shevchuk, I.V., Kuznetsov, A.V., Iwanisov, L.T.: Symmetry of turbulent boundary layer flows: investigation of different Eddy viscosity models. Acta Mech. **151**, 1–14 (2001)

Chamkha, A.J., Khaled, A.-R.A.: Similarity for hydromagnetic mixed convection heat and mass transfer for Hiemenz flow through porous media. Int. J. Numer. Methods Heat Fluid Flow **10**, 94–115 (2000)

Chamkha, A.J., Khaled, A.-R.A.: Similarity solutions for hydro magnetic simultaneous heat and mass transfer. Heat Mass Transf. **37**, 117–125 (2001)

Bluman, G.W., Kumei, S.: Symmetries and Differential Equations. Springer, New York (1989)

Birkoff, G.: Mathematics for engineers. J. Electr. Eng. **67**, 1185 (1948)

Birkoff, G.: Hydrodynamics. Princeton University Press, New Jersey (1960)

Brewster, M.Q.: Thermal Radiative Transfer Properties. Wiley, New York (1972)

Buongiorno, J.: Convective transport in nanofluids. ASME J. Heat Transf. **128**, 240–250 (2006)

Buongiorno J., Hu W.: Nanofluid coolants for advanced nuclear power plants. In: Proceedings of ICAPP '05, Seoul, 15–19, Paper no. 5705 (2005)

Cheng, W.T., Lin, H.T.: Non-similarity solution and correlation of transient heat transfer in laminar boundary layer flow over a wedge. Int. J. Eng. Sci. **40**, 531–540 (2002)

Cheng, P., Minkowycz, W.: Free convection about a vertical flat plate embedded in a porous medium with application to heat transfer from a dike. J. Geophys. Res. **82**, 2040–2044 (1977)

Choi, S.: Enhancing thermal conductivity of fluids with nanoparticle. In: Siginer, D.A., Wang, H.P. (eds.) Developments and Applications of Non-Newtonian Flows. ASME MD, vol. 231 and FED, vol. 66, pp. 99–105 (1995)

Fathalah, K.A., Elsayed, M.M.: Natural convection due to solar radiation over a non absorbing plate with and without heat losses. Int. J. Heat Fluid Flow **2**, 41–45 (1980)

Gill, S.: A process for the step-by-step integration of differential equations in an automatic digital computing machine. Proc. Cambr. Philos. Soc. **47**, 96–108 (1951)

Hakiem, M.A.E.L., Mohammadeian, A.A., Kaheir, S.M.M.E.L., Gorla, R.S.R.: Joule heating effects on MHD free convection flow of a micro polar fluid. Int. Comms. Heat Mass Transf. **26**, 219–226 (1999)

Hiemenz, K.: Die Grenzschicht an einem in den gleichfoÈrmigen FluÈssigkeitsstrom eingetauchten geraden Kreiszylinder. Dingl. Poltechnol. J. **326**, 321–410 (1911)

Hossian, M.A.: Viscous and Joule heating effects on MHD free convection flow with variable plate temperature. Int. J. Heat Mass Transf. **35**, 3485–3492 (1992)

Hunt, A.J.: Small particle heat exchangers. Lawrence Berkeley Laboratory Report No. LBL-7841. J. Renew. Sustain. Energy (1978)

Ibragimov, N.H.: Elementary Lie Group Analysis and Ordinary Differential Equations. Wiley, New York (1999)

Kafoussias, N.G., Nanousis, N.D.: Magnetohydrodynamic laminar boundary layer flow over a wedge with suction or injection. Can. J. Phys. **75**, 733 (1997a)

Kafoussias, N.G., Nanousis, N.D.: Magnetohydrodynamic laminar boundary layer flow over a wedge with suction or injection. Can. J. Phys. **75**, 733–781 (1997b)

Kandasamy, R., Loganathan, P., Puvi Arasu, P.: Scaling group transformation for MHD boundary-layer flow of a nanofluid past a vertical stretching surface in the presence of suction/injection. Nucl. Eng. Des. **241**, 2053–2059 (2011)

Kuo, B.-L.: Heat transfer analysis for the Falkner-Skan wedge flow by the differential transformation method. Int. J. Heat Mass Transf. **48**, 5036–5042 (2005)

Kuznetsov, A.V., Nield, D.A.: Natural convective boundary-layer flow of a nanofluid past a vertical plate. Int. J. Therm. Sci. **49**, 243–247 (2010)

Lai, F.C., Kulacki, F.A.: The influence of lateral mass flux on mixed convection over inclined surface in saturated porous media. ASME J. Heat Transf. **21**, 515–518 (1990)

Maxwell, J.C.: A Treatise on Electricity and Magnetism: Unabridged, vol. 2, 3rd edn. Clarendon Press, Oxford (1891)

Nakayama, A., Koyama, H.: Hitoshi Similarity solutions for buoyancy induced flows over a non-isothermal curved surface in a thermally stratified porous medium. Appl. Sci. Res. **46**, 309–314 (1989)

Nield, D.A., Kuznetsov, A.V.: The Cheng-Minkowycz problem for natural convective boundary layer flow in a porous medium saturated by a nanofluid. Int. J. Heat Mass Transf. **52**, 5792–5795 (2009)
Ovsiannikov, L.V.: Group Analysis of Differential Equations. Academic Press, New York (1982)
Oztop, H.F., Abu-Nada, E.: Numerical study of natural convection in partially heated rectangular enclosures filled with nanofluids. Int. J. Heat Fluid Flow **29**, 1326–1336 (2008)
Rana, R., Bhargava, R.: Numerical study of heat transfer enhancement in mixed convection flow along a vertical plate with heat source/sink utilizing nanofluids. Commun. Nonlinear Sci. Numer. Simul. **16**, 4318–4334 (2011)
Raptis, A.: Radiation and free convection flow through a porous medium. Int. Commun. Heat Mass Transf. **25**, 289–295 (1998)
Rosmila, A.-K., Kandasamy, K., Muhaimin, I.: Scaling group transformation for boundary-layer flow of a nanofluid past a porous vertical stretching surface in the presence of chemical reaction with heat radiation. Comput. Fluids **52**, 15–21 (2011)
Schlichting, H.: Boundary Layer Theory, vol. 9, pp. 164–165. McGraw Hill Inc, New York (1979)
Seddeek, M.A., Darwish, A.A., Abdelmeguid, M.S.: Effects of chemical reaction and variable viscosity on hydromagnetic mixed convection heat and mass transfer for Hiemenz flow through porous media with radiation. Commun. Nonlinear Sci. Numer. Simul. **12**, 195–213 (2007)
Sharma, A., Tyagi, V.V., Chen, C.R., Buddhi, D.: Review on thermal energy storage with phase change materials and applications. Renew. Sustain. Energy Rev. **13**, 318–345 (2009)
Sparrow, E.M., Cess, R.D.: Radiation Heat Transfer. Hemisphere, Washington (1978)
Tien, C.L., Hong, J.T. et al.: Natural convection in porous media under non-Darcian and non-uniform permeability conditions. In: Kakac, S. (ed.) Natural Convection, Hemisphere, Washington (1985)
Tsai, R., Huang, J.S.: Heat and mass transfer for Soret and Dufour's effects on Hiemenz flow through porous medium onto a stretching surface. Int. J. Heat Mass Transf. **52**, 2399–2406 (2009)
Vafai, K., Alkire, R.L., Tien, C.L.: An experimental investigation of heat transfer in variable porosity media. ASME J. Heat Transf. **107**, 642–647 (1985)
Vajravelu, K., Prasad, K.V., Jinho, L., Changhoon, L., Pop, I., Van Gorder, R.A.: Convective heat transfer in the flow of viscous Ag-water and cu-water nanofluids over a stretching surface. Int. J. Therm. Sci. **50**, 843–851 (2011)
Watanabe, T.: Thermal boundary layer over a wedge with uniform suction or injection in forced flow. Acta Mech. **83**, 119–126 (1990)
Yih, K.A.: The effect of uniform suction/blowing on heat transfer of Magnetohydrodynamic Hiemenz flow through porous media. Acta Mech. **130**, 147–158 (1998)
Yurusoy, M., Pakdemirli, M.: Symmetry reductions of unsteady three-dimensional boundary layers of some non-Newtonian Fluids. Int. J. Eng. Sci. **35**, 731–740 (1997)
Yurusoy, M., Pakdemirli, M.: Exact solutions of boundary layer equations of a special non-Newtonian fluid over a stretching sheet. Mech. Res. Commun. **26**, 171–175 (1999a)
Yurusoy, M., Pakdemirli, M.: Group classification of a non-Newtonian fluid model using classical approach and equivalence transformations. Int. J. Non-Linear Mech. **34**, 341–346 (1999b)
Yurusoy, M., Pakdemirli, M., Noyan, O.F.: Lie group analysis of creeping flow of a second grade fluid. Int. J. Non-Linear Mech. **36**, 955–960 (2001)